HHS Public Access

Author manuscript

Cell Stem Cell. Author manuscript; available in PMC 2017 February 04.

Published in final edited form as:

Cell Stem Cell. 2016 February 4; 18(2): 276–290. doi:10.1016/j.stem.2015.11.004.

Regulation of ribosome biogenesis and protein synthesis controls germline stem cell differentiation

Carlos G. Sanchez[1,4], **Felipe Karam Teixeira**[1,4,*], **Benjamin Czech**[2], **Jonathan B. Preall**[2], **Andrea L. Zamparini**[1], **Jessica R. K. Seifert**[1,3], **Colin D. Malone**[1], **Gregory J. Hannon**[2], and **Ruth Lehmann**[1,*]

[1]Howard Hughes Medical Institute (HHMI) and Kimmel Center for Biology and Medicine of the Skirball Institute, Department of Cell Biology, New York University School of Medicine, New York, NY 10016, USA

[2]Watson School of Biological Sciences, HHMI, Cold Spring Harbor Laboratory, Cold Spring Harbor, New York 11724, USA

[3]Department of Biology, Farmingdale State College, State University of New York, Farmingdale, New York, 11735 USA

SUMMARY

Complex regulatory networks regulate stem cell behavior and contributions to tissue growth, repair, and homeostasis. A full understanding of the networks controlling stem cell self-renewal and differentiation, however, has not yet been realized. To systematically dissect these networks and identify their components, we performed an unbiased, transcriptome-wide in vivo RNAi screen in female Drosophila germline stem cells (GSCs). Based on characterized cellular defects, we classified 646 identified genes into phenotypic and functional groups, and unveiled a comprehensive set of networks regulating GSC maintenance, survival, and differentiation. This analysis revealed an unexpected role for ribosomal assembly factors in controlling stem cell cytokinesis. Moreover, our data show that the transition from self-renewal to differentiation relies on enhanced ribosome biogenesis accompanied by increased protein synthesis. Collectively, these results detail the extensive genetic networks that control stem cell homeostasis and highlights intricate regulation of protein synthesis during differentiation.

Graphical Abstract

*Correspondence: Ruth.Lehmann@med.nyu.edu and Felipe.Teixeira@med.nyu.edu.
[4]Co-first authors

AUTHOR CONTRIBUTIONS

CGS, FKT, BC, JBP, GJH and RL designed the experiments. BC and JBP performed the primary screen. CGS performed the secondary screen, with help from ALZ, JRKS, FKT, and CDM. FKT performed bioinformatics analysis. FKT and CGS acquired the confocal images and performed all further analyses. FKT, CGS, and RL wrote the manuscript, with all authors approving the final version.

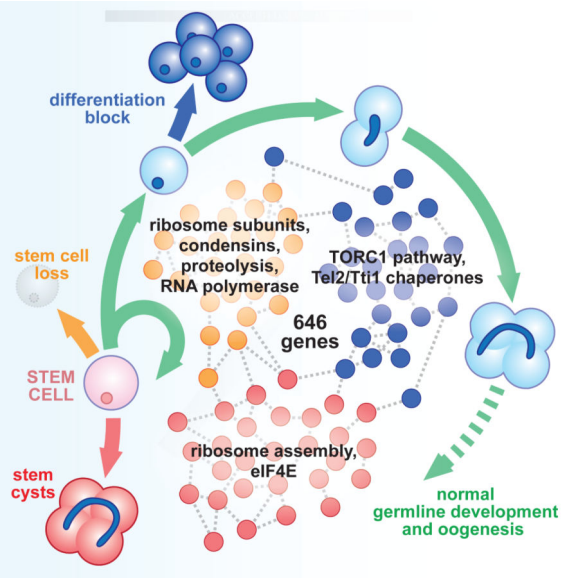

INTRODUCTION

Stem cell maintenance, as well as the control of self-renewal and differentiation is essential for proper development. For instance, stem cell ablation can lead to organ malformation and tissue replacement defects. The same is true for unbalanced shifts between stem cell self-renewal and differentiation, which can directly affect tissue architecture and may lead to tumorigenesis (Morrison and Spradling, 2008). Despite stem cell identity and commitment to differentiate being tightly controlled during development, our understanding of the intrinsic mechanisms governing these processes remains limited.

The Drosophila ovary provides an ideal system to study many aspects of stem cell biology *in vivo* (Spradling et al., 2011). Morphological and cytological features make it easy to recognize germline stem cells (GSCs) and their progeny as these differentiate. Moreover, genetic and molecular tools made available in the last two decades have proven instrumental to study germline development. Structurally, each adult ovary is composed of 12-16 independent units known as ovarioles. At the anterior tip of each ovariole, 2-3 GSCs reside adjacent to somatic niche cells (Figure 1A), which provide short-range signals essential for GSC maintenance and self-renewal. Upon GSC asymmetric cell division, the daughter cell closer to the niche retains its stem cell identity while the other cell, known as the cystoblast (CB), differentiates. As it moves away from the niche through the germarium, the CB proceeds along the differentiation path by undergoing four rounds of synchronous mitotic divisions with incomplete cytokinesis, resulting in a 16-cell interconnected germline cyst. This 16-cell cyst is then encapsulated by follicle cells and matures to an egg chamber with 15 nurse cells supporting development of the oocyte into a mature egg (Spradling et al., 2011).

Most genes known to be required for GSC maintenance and differentiation were isolated in screens for recessive mutations that lead to sterile homozygous adults (Cooley et al., 1988;

McKearin and Spradling, 1990; Schupbach and Wieschaus, 1991). However, this approach precluded the identification of genes required for animal's development or survival. Transgenic RNA interference (RNAi) resources in Drosophila have proven efficient for large-scale *in vivo* studies because of the ability to induce tissue-specific knockdown without disrupting overall animal development (Dietzl et al., 2007; Ni et al., 2011). While this approach has been applied to study germline development on a limited scale (Jankovics et al., 2014; Yan et al., 2014), unbiased screens to identify GSC maintenance and differentiation factors have not been described. Here we report a systematic, transcriptome-wide *in vivo* RNAi screen in the Drosophila germline. Careful phenotypic characterization coupled with bioinformatic analysis uncovered pathways involved in transcription, translation, protein metabolism, cell cycle progression, chromosome structure, nucleolus metabolism, cell growth, and mitochondrial cristae formation. Moreover, our analysis revealed that the transition between self-renewal and differentiation relies on the regulation of ribosome biogenesis and protein synthesis. Altogether, our screening effort has allowed us to compile the largest catalog of GSC gene networks to date. We provide a framework to understand the Drosophila GSC system as well as new insight for future experimentation in other animal stem cell systems.

RESULTS

Transcriptome-wide, *in vivo* RNAi screen identifies 646 genes required for germline development

To identify gene networks that regulate GSC maintenance or differentiation, we performed a systematic RNAi screen *in vivo*. We used *UAS-RNAi* transgenic lines from the Vienna Drosophila RNAi Center (VDRC) together with the germline specific driver *nanos-Gal4*, which is strongly expressed in GSCs and differentiating progeny (Figure S1A; Barrett et al., 1997; Dietzl et al., 2007). Efficiency of RNAi knockdown was maximized by simultaneously over-expressing the RNAi processing factor Dicer-2 (*UASDcr2*; Wang and Elgin, 2011). Additionally, we used RNA-seq analysis to limit our screening efforts to 8396 genes expressed in adult ovaries, of which *UAS-RNAi* lines targeting 8171 genes (97.3%) were available at VDRC (Table S1; Czech et al., 2013).

UAS-RNAi lines were individually crossed to *UAS-Dcr2;nanos-Gal4* flies, and F1 female progeny were visually assessed for efficacy of egg laying/hatching (Figure 1B). While the majority of the lines exhibited no or marginal alterations (7374 or 90.3%), knockdown of 797 (9.8%) genes induced a reduction in egg laying or hatching. Of these, 382 were classified as ‘no egg/larvae’, 199 as ‘few eggs/larvae’, and 216 exhibited intermediate levels of eggs/larvae (Figure S1B). To assess germline integrity by independent means, RNAs from whole F1 female flies were subjected to TaqMan qPCR assays to detect changes in the expression of two germline-specific genes (*nos* and*yTub37c*) and a ubiquitously expressed control (*Rp49*, also known as RpL32; Czech et al., 2013). The qPCR data were used to calculate Z-scores, which roughly reflect the amount of germline tissue per fly (where higher Z-score values indicate germline ablation). Knockdown of 579 genes resulted in average Z-score value higher than 1 (Figure S1C), with 493 of these (85.1%) also scoring in

the egg laying/hatching assay (Figure 1C). Combining both approaches we identified 883 candidates (hit rate of 10.8%) in the primary screen.

To characterize the cellular defects in our primary candidates, we performed a secondary screen by dissecting F1 progeny ovaries and performing immunofluorescence analysis using α-Vasa (germ cells) and α-1B1 antibodies (somatic cell membranes, spectrosomes, and fusomes; Figure 1D). For each candidate, >100 ovarioles were individually scored and classified into four hierarchical categories presented in figure 1D-E: 'no germline' (ovarioles with no Vasa-positive cells), 'germarium defects' (germline developmental defects observed within the germarium), 'egg chamber defects' (developmental alterations mainly observed upon cyst encapsulation), and 'no defect'. For each candidate, immunofluorescent data were used to quantify phenotypic frequencies and results were plotted as heatmaps (Figure 1F-H and Table S1). Such 'per germarium' analysis not only allowed us to determine the penetrance of defects, but also enabled us to classify genes into comprehensive groups (Figure 1I). For instance, candidates for which >80% of ovarioles showed no developmental alteration ('no defect') were re-grouped into the 'no phenotype' class (218 genes or 25% of primary candidates). For the 646 candidates showing development defects, we used a penetrance cutoff of >60% to organize them into the following classes: 'GSC loss' (scored as 'no germline'; 324 genes); 'early differentiation defects' (scored as 'germarium defects'; 127 genes); and 'late differentiation defects' (scored as 'egg chamber defects'; 24 genes). To these classes, we appended 'low penetrance' candidates (20-60% of defective ovarioles) exclusively scoring for a given phenotypic category (33 'GSC loss'; 34 'early differentiation'; and 30 'late differentiation'). Finally, the remaining 74 genes were grouped separately as these affected germline development in a pleiotropic manner. Knockdowns using independent *UAS-RNAi* lines allowed us to confirm the requirement for more than 75 genes (Table S1), and immunofluorescence analysis confirmed knockdown efficiency for a number of screened genes (Figure S2).

Altogether, our screen identified 646 genes required for germline development. Direct comparison to an earlier, limited screen revealed that these contain more than 450 new genes (Figure S1D; Yan et al., 2014). Genomic analysis indicated that the identified genes were evenly dispersed across the euchromatic chromosome arms and had gene length distribution similar to the entire set of screened genes (Figure S1E-F). On the other hand, we observed that the 646 hits were enriched for genes with moderate to high expression levels in adult ovaries (Figure 2A-C). This was most evident when screened genes were distributed into bins based on their expression level (ten bins, each containing 804 genes; Figure 2A) and the number of hits per bin was determined (Figure 2B). Further analysis revealed that while genes in the 'GSC loss' group were disproportionally found among the top expressed genes, those genes affecting germline differentiation tended to be more evenly distributed through moderate and high expression bins (Figure 2C).

Basic cellular machineries are enriched among genes required for germline maintenance and survival

To identify complexes and networks involved in defined developmental processes, phenotypic groups were analyzed using bioinformatics tools including COMPLEAT

(Vinayagam et al., 2013), Gene Ontology (GO), and Kyoto Encyclopedia of Genes and Genomes (KEGG). Bioinformatic analysis conducted with the 'GSC loss' group led us to identify several protein complexes required for germline maintenance (Figure 2D and S3, Table S2). Many of these complexes were involved in core cellular processes, namely transcription (RNA polymerases and splicing), translation (ribosome and translation initiation), protein metabolism (proteolysis and TCP1 chaperonin), cell cycle progression (DNA polymerase primase and spindle organization), and chromosome structure (telomere maintenance and 13S Condensin). Based on the severe phenotypic outcomes and high-expression enrichment, the bulk of the 'GSC loss' genes are likely required in many cell types in addition to the germline. To test this hypothesis, we compared 'GSC loss' genes to those leading to rudimentary ovarian morphology when knocked down in somatic ovarian cells (Handler et al., 2013). Indeed, 71% of 'GSC loss' genes were essential in both germline and somatic ovarian cells (Figure 2E), most likely relating to their function in promoting cell viability.

The frequency of 'GSC loss' hits per protein complex suggested a highly robust screening output. For instance, knockdown of every known component of the 13S Condensin or eIF3 translation initiation complexes individually induced a 'GSC loss' phenotype. The same trend was observed for larger networks, as 65 out of 79 (~82%) ribosome subunits screened were associated with germline loss (Figure 2D), validating the completeness of the screen and efficiency of RNAi knockdown.

Complete abscission of GSC daughters requires ribosome assembly factors and specific translation initiation factors

We next analyzed the set of genes affecting germline differentiation and compared the enriched networks to those obtained for the 'GSC loss' group. First, marginal overlap indicated that the phenotypic groups were composed of functionally distinct gene sets (Table S2). Second, GO analysis pointed to a strong enrichment of ribosome assembly factors among genes involved in differentiation, which contrasts with the fact that knockdown of most ribosome subunits and genes involved in rRNA transcription (RNA polymerase I complex, Figure S3) induced a 'GSC loss' phenotype (Figure 3A-B, Table S2). Ribosome assembly takes place primarily within the nucleolus before completion in the cytoplasm, and involves many non-ribosomal proteins. The process includes the transcription, processing and folding of ribosomal RNA (rRNA), its assembly into ribosomal proteins and shuttling between the nucleus and the cytoplasm (Woolford and Baserga, 2013). In addition to the strong enrichment of pre-90S components (Figure 3B), COMPLEAT analysis identified the box H/ACA small nucleolar ribonucleoprotein (snoRNP), which mediates site-specific pseudouridylation required for rRNA folding, as a top enriched complex in the differentiation group (p=1.94e^{-17}; Figure 2D and Table S2). In contrast to their yeast and mammals homologs however, the role of Drosophila ribosome assembly genes in rRNA processing remains poorly characterized. This prompted us to characterize a number of the identified candidates at the molecular level.

To do so, we knocked down ribosome assembly genes including snoRNP, pre-90S, pre-60S and pre-40S components in S2 cells and assessed the accumulation of rRNA intermediates

by northern blot analysis (Figure S4). A diversity of aberrantly accumulated rRNA intermediates was observed for 8 out of the 9 genes tested. These results not only confirm that these candidates take part in ribosome biogenesis, but also suggest that a more general rRNA processing defect underlies the differentiation defects.

To better characterize the developmental defects induced by the knockdown of ribosome assembly factors, we performed immunofluorescence analysis in the presence of a green fluorescent protein fusion (BamP-GFP; Chen and McKearin, 2003a) reporting the transcriptional activity of the differentiation factor Bag-of-marbles (Bam; McKearin and Spradling, 1990). Bam is transcriptionally regulated via a Bone Morphogenic Protein (BMP)-like signaling pathway, being repressed in GSCs and upregulated in CBs and dividing cystocytes (Figure 3C; Chen and McKearin, 2003a, b). Despite their functional diversity, knockdown of ribosome assembly factors consistently led to ovarioles containing fewer germ cells, a majority of which accumulated at the anterior tip of the ovary, adjacent to the somatic niche (Figure 3C). Absence or faint expression of the BamP-GFP reporter suggested an accumulation of undifferentiated germ cells. Robust BamP-GFP expression was only observed in a few germaria and was restricted to germ cells positioned away from the niche. Moreover, clusters of cells that were enveloped by somatic follicle cells formed abnormal egg chambers that lacked a defined oocyte (data not shown), indicating that germline development was broadly affected in these knockdowns.

In wild-type ovaries, GSCs and CBs are characterized by the presence of round, α-1B1-labeled structures called spectrosomes (Lin et al., 1994). During cyst development these cytoplasmic structures elongate and branch, becoming fusomes (Figure 1A). This morphological transition has been used to visualize germline development, and mutations blocking GSC differentiation, such as *bam*, lead to the accumulation of spectrosome-containing cells independent of their proximity to the niche (Chen and McKearin, 2003b). In knockdowns of ribosome assembly factors however, α-1B1 labeling revealed that the BamP-GFP negative germ cells found at the anterior tip of the ovary were connected to each other by elongated structures presenting characteristics of both spectrosomes and fusomes (Figure 3C, grayscale panels). It was common to observe round-shape, spectrosome-like structures within cells adjacent to the niche branching into neighboring germ cells. Within the latter cells, the α-1B1-labeled structures often adopted a terminal round shape. In their overall shape however, such extended structures were reminiscent of fusomes. Notably, these fusome-like structures varied in length, were thicker than their wild-type counterparts, and were commonly distributed perpendicularly to the niche. Interestingly, germline knockdown of eIF4E, eIF2Bα, and eIF2Bβ (Figure 3C and S5A), translation initiation factors known to modulate the efficiency of ribosome recruitment to mRNAs, also induced the formation of stereotyped fusome-like structures observed in the knockdown of ribosome assembly genes.

The presence of fusome-like structures in the ribosome assembly knockdowns implied that undifferentiated germ cells were connected to each other. In wild-type germ cells, stable cytoplasmic bridges known as ring canals are formed away from the niche during cystocyte differentiation (Figure 3D), as a consequence of incomplete cycles of cytokinesis (Robinson et al., 1994). In the knockdowns of ribosome assembly factors, we observed stable ring

canals connecting BamP-GFP negative cells that were adjacent to the somatic niche (Figure 3D). In some germaria, the phosphorylated form of the transcription factor Mothers-against-Dpp (pMAD), a classic GSC marker (Kai and Spradling, 2003), was restricted to the nucleus of the germ cell in direct contact with the niche (Figure S5B). Rarely observed in $bam^{\Delta 86}$ mutant ovaries, stable cytoplasmic bridges with trans-passing fusome-like structures that connect multiple germ cells were systematically observed when $bam^{\Delta 86}$ was combined with the knockdown of ribosome assembly factors or eIF4E (Figure 4A). Together, our results indicate that the reduction of ribosome assembly components and translation initiation factors such as eIF4E induce the formation of undifferentiated, interconnected cells.

The observed phenotype is reminiscent of 'stem cysts' that form when cytokinesis between GSC daughters is disturbed (Mathieu et al., 2013). Previous work has shown that the speed and outcome of GSC abscission, the last step of cytokinesis leading to physical separation of the two daughter cells, involves the activity of the Endosomal Sorting Complex Required for Transport-III (ESCRT-III) and is regulated by the Chromosomal Passenger Complex (CPC) and Cyclin B (Eikenes et al., 2015; Mathieu et al., 2013; Matias et al., 2015). For instance, increased activity of the CPC subunit Aurora B kinase as well as decreased levels of the ESCRT-III members such as Shrub (CHMP4) or ALIX delays abscission in GSCs, leading to the appearance of 'stem cysts' and the formation of abnormal egg chambers containing 32 cells. Remarkably, reduction of Shrb levels in $bam^{\Delta 86}$ mutants was sufficient to induce the formation of stable cytoplasmic bridges with trans-passing fusome-like structures (Figure 4A). Given the phenotypic similarities, we investigated whether the ribosome assembly/translation initiation and the CPC/ESCRTIII abscission pathways are functionally linked. Using the frequency of 32-cell egg chambers as a readout for delay in GSC abscission (Figure 4B-C), we performed genetic interaction experiments combining mutations in ribosome assembly factors or eIF4E with those in Shrub. Some egg chambers containing 32 cells were always observed in heterozygous *shrb* alleles as previously described (Figure 4D; Matias et al., 2015), while 32-cell egg chambers were rarely observed in heterozygous mutants for eIF4E or ribosome assembly factors alone. In contrast, simultaneously lowering the levels of eIF4E and Shrub by combining mutant alleles in double heterozygous flies led to a significant increase in the frequency of 32-cell egg chamber when compared to their single heterozygous siblings. We also observed an increase in the frequency of 32-cell egg chambers when Shrb alleles were combined with a mutation affecting the box H/ACA snoRNP subunit DKC1 (Nop60B; Giordano et al., 1999) or with a P-element insertion into the pre-60S factor MTR4 (RpLP0-like; Figure S5D), suggesting that ribosome assembly factors and eIF4E interact positively with the ESCRT-III protein Shrb to promote GSC abscission. Additionally, our results suggest that ribosome assembly and eIF4E are also required for overall growth, given the reduced number and eventual loss of germ cells in these knockdowns.

The TORC1 pathway and the cochaperone adaptor complex Tel2/Tti1 are required for GSC differentiation

Many of the ribosome assembly factors identified in our screen were previously shown to be downregulated in Drosophila cultured cells treated with rapamycin (Guertin et al., 2006). Rapamycin is a small molecule that directly inhibits the activity of the Target of Rapamycin

(TOR) kinase, the central component of the signaling pathway that controls many aspects of cell growth and proliferation in response to inputs such as insulin, growth factors, and amino acids (Laplante and Sabatini, 2009). Previous studies established a role for insulin signaling and dTOR in regulating GSC maintenance and proliferation (Hsu et al., 2008; LaFever et al., 2010). KEGG analysis on genes affecting differentiation identified 'mTOR signaling' as an enriched pathway ($p = 1.92e^{-01}$; Table S2). Further analysis revealed that the pyruvate dehydrogenase kinase (Pdk), the v-akt murine thymoma viral oncogene homologue 1 kinase (dAkt1), the TOR kinase (dTOR), the regulatory associated protein of mTOR (dRaptor), and the cytoplasmic insulin receptor substrate (dIRS/chico) were required for germline differentiation (Figure 5A; Yan et al., 2014). Moreover, knockdown of the cochaperone adaptors Telomerase Maintenance 2 homolog/liquid facets-Related (dTel2/lqfR; Lee and Fischer, 2012) and TEL2 Interacting Protein 1 homolog (dTti1/CG16908; Glatter et al., 2011), which are essential for the stability and functioning of the TOR kinase (Kaizuka et al., 2010; Takai et al., 2007), induced differentiation defects (Figure 5A). Immunofluorescence analysis revealed that knockdown of factors participating in the TOR pathway primarily caused a block in differentiation and growth, leading to a limited accumulation of spectrosome-containing, undifferentiated germ cells (Figure 5A). While germ cells attached to the niche did not express the BamP-GFP reporter, those located further away displayed weak to intermediate GFP expression. For the insulin receptor substrate dIRS/chico, we also observed an accumulation of partially differentiated, BamP-GFP positive, fusome-containing cysts towards the posterior end of the germaria, which were rarely capable of developing into normal egg chambers. Most post-germarium chambers in TOR pathway knockdowns were composed of undifferentiated or partially differentiated germ cells surrounded by somatic follicle cells (Figure 5A). Despite some variability, the differentiation defects induced by the germline knockdown of components involved in TOR signaling did not phenocopy those observed for ribosome assembly factors (compare figure 3C and 5A). Taken together, these results suggest that in addition to its established role in GSC maintenance (Hsu et al., 2008; LaFever et al., 2010), the TOR signaling pathway, including the Drosophila Tel2-Tti1-TOR complex (dTTT, Figure 2D; Glatter et al., 2011), is required for germline differentiation independent of its role in promoting the expression of ribosome assembly factors.

The cochaperone adaptor dTel2/dTti1 is required for growth and nucleolar hypertrophy in GSCs

The TOR pathway is known to modulate growth by regulating protein synthesis at multiple levels including rRNA transcription, ribosome assembly, and initiation of translation (Laplante and Sabatini, 2009). In the Drosophila germline, rRNA transcription rate was recently shown to positively modulate stem cell proliferation and maintenance (Zhang et al., 2014). Remarkably, GSCs possess enlarged nucleoli and concurrent high levels of rRNA transcription (Neumuller et al., 2008; Zhang et al., 2014). Nucleolar size and rRNA transcription decreases progressively during germline differentiation, reaching lowest levels during 16-cell cyst formation (Figure 5C). Increased rRNA transcription is re-established during egg chamber formation, paralleling an enlarged nucleolar size in endoreplicating nurse cells (Neumuller et al., 2008; Zhang et al., 2014). Given its role in promoting growth via rRNA transcription, we tested whether TOR activity underlies nucleolar hypertrophy in

GSCs. Using the well-characterized α-fibrillarin antibody as a nucleolus marker, we acquired optical sections and reconstructed 3D images to determine nucleolar volume in various knockdowns. Our analysis indicated that knockdown of the core components of the TORC1 signaling pathway (dTOR and dRaptor) mildly affected GSC nucleolar volume (15-20% reduction) when compared to control (Figure 5B, 5D). Consistent with the role of TORC1 in promoting cell growth (Guertin et al., 2006; Laplante and Sabatini, 2009), this reduction was accompanied by a similar decrease in nuclear volume, as determined by DAPI staining. Of note, BamP-GFP negative germ cells found within the germaria of these knockdowns showed enlarged nucleoli regardless of their position with respect to the niche (Figure 5B). Interestingly, this was also the case for the knockdown of ribosome assembly factors NOB1 (Figure 5B and D), DKC1, GAR1, and NOP10 (Figure S5C), attesting to the undifferentiated state of 'stem cysts'. Surprisingly, knockdown of the cochaperone adaptors dTel2 and dTti1 strongly reduced nucleolar volume in all germ cells, including those adjacent to the niche (>50% reduction, Figure 5B and 5D). The observed effect on nucleolar volume was not paralleled by an equivalent reduction in nuclear volume. Therefore, and in addition to its role in stabilizing the TOR kinase, these results suggest that the cochaperone adaptor complex Tel2/Tti1 regulates rRNA synthesis in germ cells through an alternative pathway.

The fact that reduced nucleolar volume is associated with germline differentiation in wild-type ovaries (Figure 5C) and that impairment of the RNA polymerase I regulatory complex was associated with premature GSC differentiation (Zhang et al., 2014) prompted us to characterize the identity of germ cells in dTel2 and dTti1 knockdowns. GSCs are defined by high levels of pMAD as well as the transcriptional activation of the Daughters against dpp (Dad) gene, which are triggered by a signaling cascade in response to the BMP ligands supplied by the somatic niche (Kai and Spradling, 2003; Tsuneizumi et al., 1997). Using a transcriptional reporter (*Dad-LacZ*, Tsuneizumi et al., 1997), we observed that germ cells adjacent to the niche showed strong Dad expression and equal elevated pMAD levels in dTel2 and dTti1 knockdowns (Figure 6A-B), further confirming their GSC identity. As germ cells moved away from the niche in these knockdowns, pMAD and Dad-LacZ levels decreased while the expression of BamP-GFP reporter increased (Figure 5A, 6A-B). Thus, our results indicate that neither niche-germline interactions nor GSC fate were affected in dTel2 and dTti1 knockdowns, and that reducing rRNA production in GSCs is not sufficient to promote differentiation. Since pMAD and Dad-LacZ regulation was unaffected, we conclude that the block in differentiation was not due to either extended or persistent BMP signaling (Figure 6A-B).

Bam functions to promote CB differentiation and thus remains transcriptionally repressed in GSCs (Chen and McKearin, 2003a, b; McKearin and Spradling, 1990). Our results suggest that the requirement for dTel2 and dTti1 precedes niche exclusion, as these were critical for nucleolar hypertrophy in GSCs (Figure 5C). To further explore these observations, we performed epistasis experiments using the $bam^{\Delta 86}$ mutant allele in combination with dTel2 and dTti1 knockdowns (Figure 6C). *bam* mutant ovaries were characterized by an over accumulation of undifferentiated germ cells containing GSC-like, enlarged nucleoli (Neumuller et al., 2008). When $bam^{\Delta 86}$ was combined with either dTel2 or dTti1

knockdowns, all germ cells showed a marked decrease in nucleolar volume. dTel2 and dTti1 knockdowns affected GSC nucleolar volume to a similar extent regardless of the *bam*$^{\Delta 86}$ mutation (Figure 5D, 6D). Moreover, we observed that knockdown of the cochaperone adaptors partially suppressed the hyperplastic nature of *bam* ovaries, with dTti1 KD;*bam*$^{\Delta 86}$ and dTel2 KD;*bam*$^{\Delta 86}$ germaria being filled with far fewer germ cells than *bam*$^{\Delta 86}$ mutants (Figure 6E). Altogether, our results indicate that the Tel2/Tti1 complex promotes growth and supports GSC differentiation program.

The dTel2/dTti1 target dTRRAP/Nipped-A affects GSC differentiation and nucleolar hypertrophy

The Tel2/Tti1 complex functions as a cochaperone adaptor presenting a specific set of client proteins to be stabilized by the molecular chaperone HSP90-R2TP (Izumi et al., 2012). Knockdown of Hsp83 (Hsp90 homolog), as well as of the R2TP cochaperone subunits Pontin (Rvb1 homolog) and Reptin (Rvb2 homolog), caused ‘GSC loss’ (Figure 2D, Table S1). In contrast, germline knockdown of the Drosophila Tah1 homolog Spaghetti (Spag; Figure S2; Benbahouche Nel et al., 2014), an exclusive component of the R2TP complex, led to the accumulation of spectrosome-containing undifferentiated germ cells (Figure 6F). This was also the case for the knockdown of CG16734, a dipteran-specific protein that directly binds to dTti1 (Glatter et al., 2011). Supporting a functional interaction with Tel2/Tti1, knockdowns of both Spag and CG16734 resulted in a decrease in GSC nucleolar volume (Figure 6G-H).

Tel2/Tti1 is required for the stability of all phosphatidylinositol 3-kinase-related kinases (PIKK), which include mTOR, ataxia telangiectasia mutated (ATM), ATM- and Rad3-related (ATR), DNA-PKcs, suppressor with morphological effect on genitalia 1 (SMG-1), and the transformation/transcription domain associated protein (TRRAP; Kaizuka et al., 2010; Takai et al., 2007). In addition to dTOR, dTRRAP (also known as Nipped-A) was the only PIKK for which differentiation defects reminiscent of dTel2 and dTti1 were observed (Figure 6F, Table S1). Given that TRRAP was shown to bind ribosomal DNA in mammalian cells (Arabi et al., 2005), we investigated the possibility of dTRRAP being required for nucleolar hypertrophy in GSCs. dTRAAP knockdown reduced nucleolar volume >50% in undifferentiated germ cells, including those adjacent to the somatic niche (Figure 6G-H). Taken together, our analysis identified a gene network that operates through the nucleolar-enriched transcription cofactor dTRRAP and that is required for GSC growth, nucleolar hypertrophy, and differentiation.

GSC differentiation is associated with increased global protein synthesis

The fact that knockdown of pathway components promoting ribosome biogenesis and protein synthesis cause an accumulation of undifferentiated germ cells suggests that the differentiation process relies on a robust translation system. To visualize global protein synthesis *in vivo*, we employed a recently developed assay that uses O-propargylpuromycin (OP-Puro), an alkyne analog of puromycin, and the click chemistry to label nascent polypeptide chains (Liu et al., 2012). Living wild-type ovaries were incubated with OP-Puro for up to 60 minutes prior to fixation, labeling, and confocal imaging (Figure 7A). Quantification of OP-Puro signal in wild-type ovaries revealed that differentiating germ

cells consistently present increased protein synthesis rate when compared to GSCs (Figure 7B and S6A). Increased OP-Puro signal was observed from 2-to 8-cell cysts, with 4-cell cysts showing maximum fluorescence intensities (Figure 7B). Interestingly, global protein synthesis rate in the germline transitorily collapsed after the completion of mitotic cell divisions, with recently formed 16-cell cysts showing low OPPuro fluorescent intensities (Figure 7A). Together, our results indicate that GSC differentiation is associated with increased global protein synthesis rate. Notably, this pattern was not restricted to the female germline, as a similar increase in global protein synthesis rate during differentiation was observed in spermatogenesis (Figure S6B). Moreover, robust increase in OP-Puro signal was abolished in $bam^{\Delta 86}$ mutant ovaries, further confirming that the increase in translation rate is part of the differentiation program (Figure 7C). Finally, by combining OP-Puro and mutant clonal analysis using previously characterized alleles (Glatter et al., 2011), we were able to confirm that dTti1 promotes global protein synthesis *in vivo*. While mutant clones were rarely observed in the germline, mosaic analysis conducted in ovarian somatic tissues revealed a dramatic decrease in protein synthesis in homozygous mutant clones compared to non-mutant neighboring cells (Figure S6C).

DISCUSSION

Using the Drosophila germline as an *in vivo* model to study stem cell biology, we performed a systematic, unbiased, transcriptome-wide RNAi screen. Out of the 8171 genes knocked down, we identified 646 to be autonomously required for germline development. To our knowledge, these make up the largest set of germline genes described so far and comprise more than 450 genes with no prior reported association to germline development (Perrimon et al., 1996; Schupbach and Wieschaus, 1991; Yan et al., 2014). Characterization through confocal analysis allowed us to determine the penetrance of germline defects induced by knockdown as well as to phenotypically classify each gene into biologically meaningful groups. The qualitative and quantitative character of such data has proven instrumental for the identification of gene networks involved in either GSCs maintenance or differentiation. Despite our efforts however, only a fraction of the newly identified genes could be allocated into known networks and many remain unexplored. Therefore, we expect our data will serve as a valuable resource for future studies in the stem cell biology field. Moreover, the fact that more than 90% of the identified genes have orthologs in mammals (Table S3) further attests to the importance of our work to stem cell research in general.

To maximize coverage while coping with the labor-intensive screening process, primary screening analysis was performed using one RNAi line per target gene. With this strategy, we were able to test more than 97% of the 8396 genes with significant expression in the adult ovary. As a consequence of our approach, we can not rule out some proportion of false negatives stemming from line-specific, ineffective RNAi. Nevertheless, results obtained for the germline knockdown of individual ribosome subunits are indicative of an efficient output (~80% efficacy), similar to what was previously reported in an RNAi screen performed in Drosophila somatic ovarian tissue (Handler et al., 2013). Testing independent RNAi lines for each target gene could attenuate false negative issues, and published data indicate that assaying a second transgenic RNAi line translates into a slightly larger number of hits (20-30%) when compared to a one line/gene approach (Dietzl et al., 2007; Handler et

al., 2013; Yan et al., 2014). In our study, the false negative rate has proven negligible for asserting network or pathway requirement through genomic analysis, although it may have impacted our ability to detect complexes composed of few genes. Based on our results and on previously published data (Figure S1E; Perrimon et al., 1996; Schupbach and Wieschaus, 1991; Yan et al., 2014), we speculate that the number of factors required for GSC maintenance and early differentiation may not exceed ~1000 genes, with a large fraction of these factors being implicated in essential cellular functions.

Our results revealed that germline knockdown of many ribosome assembly components and key translation initiation factors led to accumulation of 'stem cysts' – clusters of undifferentiated cells found adjacent to the niche and connected to each other through cytoplasmic bridges (Figure 7D). At the molecular level, inhibition of the ribosome biogenesis pathway elicits the assembly of functionally altered ribosomes. For instance, mutations in the box H/ACA snoRNP catalytic subunit DKC1 affect translation fidelity and internal ribosomal entry sites (IRES)-dependent translation in yeast and in mammals (Jack et al., 2011). How the activity of the translational apparatus affects the fate of the cytokinetic furrow in germ cells remains to be determined. Given the observed functional interaction with the CPC/ESCRT-III pathway (Eikenes et al., 2015; Mathieu et al., 2013; Matias et al., 2015), one exciting possibility is that abscission factors are exquisitely sensitive to the status of the translation machinery. Compelling evidence for targeted regulation was recently provided by the characterization of eIF4E haploinsufficient mice, which revealed that eIF4E levels are critical for the translation of a subset of transcripts during oncogenic transformation (Truitt et al., 2015). It is tempting to speculate that during germline development, stabilization of the arrested furrows involves a specialized form of translational control. Indeed, mounting evidence suggests that changes in ribosome function govern key developmental processes (Xue and Barna, 2012).

The undifferentiated state of the fusome-containing 'stem cyst' challenges the prevailing notion that the transition between round spectrosome and elongated fusome is an absolute mark of germ cell differentiation. Previous reports relied on this transition to propose the existence of a Bam-independent differentiation pathway triggered by reduced rRNA transcription or translation activity (Xi et al., 2005; Zhang et al., 2014). Supporting this hypothesis was the fact that fusome-containing cysts accumulate in $bam^{\Delta 86}$ mutant when this is combined with mutations affecting either the translational release factor-like protein Pelota (*pelo*; Xi et al., 2005) or the Drosophila-specific RNA polymerase I cofactor Under-developed (*udd*; Zhang et al., 2014). In the light of our findings, we propose that the reported phenotype can be alternatively explained by the effect of ribosome assembly and translational machineries on abscission, independent of germ cell differentiation. Interestingly, the uncoupling of germline differentiation and incomplete cytokinesis also infers that mechanisms must exist to ensure proper abscission between GSC daughters in wild-type conditions (Eikenes et al., 2015; Mathieu et al., 2013; Matias et al., 2015). While it is known that the GSC stays attached to future CB until the G2 phase of the following cell cycle (de Cuevas and Spradling, 1998), what regulates this uncommon abscission process remains elusive.

Finally, our results revealed a central role for nucleolus functioning and protein synthesis in GSC biology (Figure 7D-E). On one hand, hyperactive ribosome biogenesis would promote stem cell growth and consequently enhance competitiveness for niche occupancy (LaFever et al., 2010; Zhang et al., 2014). Paradoxically, evidence suggests that enhanced nucleolus activity and concurrent growth is regulated independently of signals provided by the niche. Indeed, *bam* mutant germ cells show nucleolar hypertrophy irrespective of their position in the germarium, and this is associated with an overproliferative phenotype related to rapid growing cancer cells (Neumuller et al., 2008). While systemic extrinsic factors promoting GSC growth remain to be characterized (Hsu et al., 2008), we uncovered a gene network that operates through the transcription cofactor dTRRAP, in addition to TOR signaling, to autonomously regulate GSC nucleolus hypertrophy and growth (Figure 7E). Interestingly, TRRAP was previously shown to support c-Myc-mediated oncogenic transformation in mammals (McMahon et al., 1998), suggesting parallels between GSCs and cancer cells. On the other hand, our analysis uncovered an essential role for TOR- and TRAAP-centered pathways during germline differentiation, with knockdowns leading to the accumulation of undifferentiated cells (GSC- and CB-like cells). Consistent with a special need for protein synthesis during critical differentiation stages, global synthesis rate is increased in differentiating cells (2- to 8-cell cysts) in comparison to GSCs. Interestingly, similar increases in protein synthesis were observed in other *in vitro* and *in vivo* somatic and embryonic stem cell differentiation systems in mammals (Ingolia et al., 2011; Sampath et al., 2008; Signer et al., 2014). Unexpectedly, however, this process correlates with a decrease in nucleolus volume as well as in rRNA transcription during GSC differentiation (this study; Neumuller et al., 2008; Zhang et al., 2014). As translation rate is generally positively correlated with rRNA synthesis, our results imply that increase in translation rate is actively regulated during differentiation by means that remain to be characterized. In this context, our observations expand the model proposed by (Zhang et al., 2014), revealing another layer of regulation that uncouples rRNA and protein synthesis during GSC differentiation. One previously alluded possibility is that enhanced rRNA synthesis in undifferentiated cells may prime differentiating daughters with an abundance of ribosomes, enough to sustain enhanced translation rate during differentiation stages (Ingolia et al., 2011). In line with this, our findings indicate that the balance between GSC self-renewal and differentiation is critically sensitive to both ribosome biogenesis and translation output levels. While accumulating evidence suggests that changes in protein synthesis rate is important for tissue homeostasis and cancer (Buszczak et al., 2014; Signer et al., 2014; Truitt et al., 2015), it will be important to elucidate the specific regulatory mechanisms underlying transitions such as those uncovered by our analysis.

EXPERIMENTAL PROCEDURES

Fly stocks and husbandry

Primary screen was performed as previously described (Czech et al., 2013). Details on fly stocks and husbandry, secondary screen, genetic interaction, and clonal analyses are provided in the Supplementary Experimental Procedures.

RNA Isolation, Reverse Transcription, and qPCR

RNA analysis during primary screen was performed as previously described (Czech et al., 2013). Fore details see Supplemental Experimental Procedures.

Immunofluorescence

Adult ovaries were immunostained according to standard procedures and images were acquired on a Zeiss LSM 780 confocal microscope. For protocols and list of primary and secondary antibodies see Supplemental Experimental Procedures.

Image handling, nucleolar and nuclear volume quantification

Nucleolar volume was determined using IMARIS ×64 software after 3D reconstructions from Z-stack images. Nuclear volume was inferred from the nuclear diameter as determined using ImageJ (NIH; http://imagej.nih.gov/ij/). A one-way analysis of variance (ANOVA, $p<0.001$) was applied to the nucleolar/nuclear volume ratios. For details see Supplemental Experimental Procedures.

Measurement of global protein synthesis *in vivo*

Protein synthesis was detected by the Click-iT® Plus OPP Alexa Fluor 594 Protein Synthesis Assay Kit (Molecular Probes). Samples were dissected in Shields and Sang M3 Insect Medium (Sigma) and immediately transferred to fresh medium containing a 1:400 dilution of Click-iT OPP Reagent (OP-puro 50 μM, final concentration). Samples were incubated at room temperature for 15, 30, 45, 60 minutes, then rinsed 3 times with PBS. For clonal analysis, samples were incubated with OPP reagent for 30 minutes. All samples were fixed with 5% formaldehyde in PBS for 20 min, washed with 0.5% Triton X-100 in PBS, and incubated for 15 min in PBS with 3% (w/v) BSA. For the Click-iT® reaction, samples were incubated in dark at room temperature in Click-iT® reaction cocktail. After 30 min, samples were washed with Click-iT® Reaction Rinse Buffer then with PBS with 3% BSA. Samples were washed with PBS with 1% BSA and 0.2% Triton X-100 for 1 hour and immunostained according to standard procedures.

Quantification of OP-Puro fluorescence intensity was performed using ImageJ (NIH; http://imagej.nih.gov/ij/). To avoid misrepresentation due to possible heterogeneous OPPuro signal distribution within a cell, we determined mean OP-Puro fluorescence intensities for two independent ‘region of interest’ (ROIs, 1.25μmx1.25μm in size) per cell. Measurements were restricted to the cytoplasm of germ cells. For each analyzed germarium, mean intensities were normalized to the average intensities observed for GSCs. Each experiment was done in duplicates. At least 6 independent germaria were analyzed per time point. A one-way analysis of variance (ANOVA, $p<0.001$) was applied to the data.

RNAi, RT-qPCR, and northern blot analyses in Drosophila S2 cells

Knockdown in S2 cells was performed by transfection of dsRNA using Qiagen's effectene reagent. Standard RNA analysis and quantitative PCR was performed to verify knockdown efficiency. Northern blot analyses were performed using previously described probes

(Giordano et al., 1999). Primers, probe sequences, and detailed procedures see Supplemental Experimental Procedures.

Bioinformatic analysis

GO and KEGG analyses were performed using DAVID (http://david.abcc.ncifcrf.gov/). The entire set of screened genes was used as experimental background. Enriched terms for the 'GSC loss' and 'differentiation' groups are displayed in Table S2, with a *p*-value filter of $p<0.05$.

Protein complex enrichment analysis was performed using COMPLEAT (http://www.flyrnai.org/compleat/). Protein complexes over-represented in genes found in 'GSC loss' and 'differentiation' groups are listed in Table S2. For the protein complexes presented in Figures 2D and S3, phenotypes of individual components were manually assigned after COMPLEAT analysis. As experimental background, we used the entire set of screened genes. Complex size was limited to >3 and <100, with a *p*-value filter of $p<0.05$.

Chromosome distribution as well as yeast, mouse, and human orthologs were determined using FlyMine (www.flymine.org). Gene length was retrieved from FlyBase (www.flybase.org). Expression data used in figure 2A is found at the Gene Expression Omnibus database under accession number GSE46101 (Czech et al., 2013).

Supplementary Material

Refer to Web version on PubMed Central for supplementary material.

ACKNOWLEDGEMENTS

We are grateful to J. Sanny and M. Okuniewska for help with fly husbandry, and to R. Cinalli for comments. We thank B. Pradet-Balade (CNRS), M. Gstaiger, H. Stocker (ETHZ), and P. Lasko (McGill University) for sharing reagents and Alexey Soshnev with design of graphical abstract. We acknowledge VDRC and BDSC for reagents. CGS is supported by NIH F31/HD080380, FKT by EMBO and HFSP fellowships, BC by a Boehringer Ingelheim Fonds PhD fellowship, JBP by ACS award 121614-PF-11-277-01-RMC, JRKS by NIH F32/GM082169, CDM by a HHWF fellowship. This work was supported by the NIH (5R01GM062534) and a gift from Kathryn W. Davis to GJH. RL is supported by NIH R01/R37HD41900. RL and GJH are HHMI investigators.

REFERENCES

Arabi A, Wu S, Ridderstrale K, Bierhoff H, Shiue C, Fatyol K, Fahlen S, Hydbring P, Soderberg O, Grummt I, et al. c-Myc associates with ribosomal DNA and activates RNA polymerase I transcription. Nat. Cell Biol. 2005; 7:303–310. [PubMed: 15723053]

Barrett K, Leptin M, Settleman J. The Rho GTPase and a putative RhoGEF mediate a signaling pathway for the cell shape changes in Drosophila gastrulation. Cell. 1997; 91:905–915. [PubMed: 9428514]

Benbahouche Nel H, Iliopoulos I, Torok I, Marhold J, Henri J, Kajava AV, Farkas R, Kempf T, Schnolzer M, Meyer P, et al. Drosophila Spag is the homolog of RNA polymerase II-associated protein 3 (RPAP3) and recruits the heat shock proteins 70 and 90 (Hsp70 and Hsp90) during the assembly of cellular machineries. J. Biol. Chem. 2014; 289:6236–6247. [PubMed: 24394412]

Buszczak M, Signer RA, Morrison SJ. Cellular differences in protein synthesis regulate tissue homeostasis. Cell. 2014; 159:242–251. [PubMed: 25303523]

Chen D, McKearin DM. A discrete transcriptional silencer in the bam gene determines asymmetric division of the Drosophila germline stem cell. Development. 2003a; 130:1159–1170. [PubMed: 12571107]

Chen D, McKearin DM. Dpp Signaling Silences bam Transcription Directly to Establish Asymmetric Divisions of Germline Stem Cells. Curr. Biol. 2003b; 13:1786–1791. [PubMed: 14561403]

Cooley L, Kelley R, Spradling AC. Insertional mutagenesis of the Drosophila genome with single P elements. Science. 1988; 239:1121–1128. [PubMed: 2830671]

Czech B, Preall JB, McGinn J, Hannon GJ. A transcriptome-wide RNAi screen in the Drosophila ovary reveals factors of the germline piRNA pathway. Mol. Cell. 2013; 50:749–761. [PubMed: 23665227]

de Cuevas M, Spradling AC. Morphogenesis of the Drosophila fusome and its implications for oocyte specification. Development. 1998; 125:2781–2789. [PubMed: 9655801]

Dietzl G, Chen D, Schnorrer F, Su KC, Barinova Y, Fellner M, Gasser B, Kinsey K, Oppel S, Scheiblauer S, et al. A genome-wide transgenic RNAi library for conditional gene inactivation in Drosophila. Nature. 2007; 448:151–156. [PubMed: 17625558]

Eikenes AH, Malerod L, Christensen AL, Steen CB, Mathieu J, Nezis IP, Liestol K, Huynh JR, Stenmark H, Haglund K. ALIX and ESCRT-III coordinately control cytokinetic abscission during germline stem cell division in vivo. PLoS Genet. 2015; 11:e1004904. [PubMed: 25635693]

Giordano E, Peluso I, Senger S, Furia M. minifly, a Drosophila gene required for ribosome biogenesis. J. Cell Biol. 1999; 144:1123–1133. [PubMed: 10087258]

Glatter T, Schittenhelm RB, Rinner O, Roguska K, Wepf A, Junger MA, Kohler K, Jevtov I, Choi H, Schmidt A, et al. Modularity and hormone sensitivity of the Drosophila melanogaster insulin receptor/target of rapamycin interaction proteome. Mol. Sys. Biol. 2011; 7:547.

Guertin DA, Guntur KV, Bell GW, Thoreen CC, Sabatini DM. Functional genomics identifies TOR-regulated genes that control growth and division. Curr. Biol. 2006; 16:958–970. [PubMed: 16713952]

Handler D, Meixner K, Pizka M, Lauss K, Schmied C, Gruber FS, Brennecke J. The genetic makeup of the Drosophila piRNA pathway. Mol. Cell50. 2013:762–777.

Hsu HJ, LaFever L, Drummond-Barbosa D. Diet controls normal and tumorous germline stem cells via insulin-dependent and -independent mechanisms in Drosophila. Dev. Biol. 2008; 313:700–712. [PubMed: 18068153]

Ingolia NT, Lareau LF, Weissman JS. Ribosome profiling of mouse embryonic stem cells reveals the complexity and dynamics of mammalian proteomes. Cell. 2011; 147:789–802. [PubMed: 22056041]

Izumi N, Yamashita A, Ohno S. Integrated regulation of PIKK-mediated stress responses by AAA+ proteins RUVBL1 and RUVBL2. Nucleus. 2012; 3:29–43. [PubMed: 22540023]

Jack K, Bellodi C, Landry DM, Niederer RO, Meskauskas A, Musalgaonkar S, Kopmar N, Krasnykh O, Dean AM, Thompson SR, et al. rRNA pseudouridylation defects affect ribosomal ligand binding and translational fidelity from yeast to human cells. Mol. Cell. 2011; 44:660–666. [PubMed: 22099312]

Jankovics F, Henn L, Bujna A, Vilmos P, Spirohn K, Boutros M, Erdelyi M. Functional analysis of the Drosophila embryonic germ cell transcriptome by RNA interference. PloS One. 2014; 9:e98579. [PubMed: 24896584]

Kai T, Spradling AC. An empty Drosophila stem cell niche reactivates the proliferation of ectopic cells. Proc. Nat. Acad. Sci. USA. 2003; 100:4633–4638. [PubMed: 12676994]

Kaizuka T, Hara T, Oshiro N, Kikkawa U, Yonezawa K, Takehana K, Iemura S, Natsume T, Mizushima N. Tti1 and Tel2 are critical factors in mammalian target of rapamycin complex assembly. J. Biol. Chem. 2010; 285:20109–20116. [PubMed: 20427287]

LaFever L, Feoktistov A, Hsu HJ, Drummond-Barbosa D. Specific roles of Target of rapamycin in the control of stem cells and their progeny in the Drosophila ovary. Development. 2010; 137:2117–2126. [PubMed: 20504961]

Laplante M, Sabatini DM. mTOR signaling at a glance. J. Cell Sci. 2009; 122:3589–3594. [PubMed: 19812304]

Lee JH, Fischer JA. Drosophila Tel2 is expressed as a translational fusion with EpsinR and is a regulator of wingless signaling. PloS One. 2012; 7:e46357. [PubMed: 23029494]

Lin H, Yue L, Spradling AC. The Drosophila fusome, a germline-specific organelle, contains membrane skeletal proteins and functions in cyst formation. Development. 1994; 120:947–956. [PubMed: 7600970]

Liu J, Xu Y, Stoleru D, Salic A. Imaging protein synthesis in cells and tissues with an alkyne analog of puromycin. Proc. Nat. Acad. Sci. USA. 2012; 109:413–418. [PubMed: 22160674]

Mathieu J, Cauvin C, Moch C, Radford SJ, Sampaio P, Perdigoto CN, Schweisguth F, Bardin AJ, Sunkel CE, McKim K, et al. Aurora B and cyclin B have opposite effects on the timing of cytokinesis abscission in Drosophila germ cells and in vertebrate somatic cells. Dev. Cell. 2013; 26:250–265. [PubMed: 23948252]

Matias NR, Mathieu J, Huynh JR. Abscission Is Regulated by the ESCRT-III Protein Shrub in Drosophila Germline Stem Cells. PLoS Genet. 2015; 11:e1004653. [PubMed: 25647097]

McKearin DM, Spradling AC. bag-of-marbles: a Drosophila gene required to initiate both male and female gametogenesis. Genes Dev. 1990; 4:2242–2251. [PubMed: 2279698]

McMahon SB, Van Buskirk HA, Dugan KA, Copeland TD, Cole MD. The novel ATM-related protein TRRAP is an essential cofactor for the c-Myc and E2F oncoproteins. Cell. 1998; 94:363–374. [PubMed: 9708738]

Morrison SJ, Spradling AC. Stem cells and niches: mechanisms that promote stem cell maintenance throughout life. Cell. 2008; 132:598–611. [PubMed: 18295578]

Neumuller RA, Betschinger J, Fischer A, Bushati N, Poernbacher I, Mechtler K, Cohen SM, Knoblich JA. Mei-P26 regulates microRNAs and cell growth in the Drosophila ovarian stem cell lineage. Nature. 2008; 454:241–245. [PubMed: 18528333]

Ni JQ, Zhou R, Czech B, Liu LP, Holderbaum L, Yang-Zhou D, Shim HS, Tao R, Handler D, Karpowicz P, et al. A genome-scale shRNA resource for transgenic RNAi in Drosophila. Nat. Methods. 2011; 8:405–407. [PubMed: 21460824]

Perrimon N, Lanjuin A, Arnold C, Noll E. Zygotic lethal mutations with maternal effect phenotypes in Drosophila melanogaster. II. Loci on the second and third chromosomes identified by P-element-induced mutations. Genetics. 1996; 144:1681–1692. [PubMed: 8978055]

Robinson DN, Cant K, Cooley L. Morphogenesis of Drosophila ovarian ring canals. Development. 1994; 120:2015–2025. [PubMed: 7925006]

Sampath P, Pritchard DK, Pabon L, Reinecke H, Schwartz SM, Morris DR, Murry CE. A hierarchical network controls protein translation during murine embryonic stem cell self-renewal and differentiation. Cell Stem Cell. 2008; 2:448–460. [PubMed: 18462695]

Schupbach T, Wieschaus E. Female sterile mutations on the second chromosome of Drosophila melanogaster. II. Mutations blocking oogenesis or altering egg morphology. Genetics. 1991; 129:1119–1136. [PubMed: 1783295]

Signer RA, Magee JA, Salic A, Morrison SJ. Haematopoietic stem cells require a highly regulated protein synthesis rate. Nature. 2014; 509:49–54. [PubMed: 24670665]

Spradling AC, Fuller MT, Braun RE, Yoshida S. Germline stem cells. Cold Spring Harb. Perspect. Biol. 2011; 3:a002642. [PubMed: 21791699]

Takai H, Wang RC, Takai KK, Yang H, de Lange T. Tel2 regulates the stability of PI3K-related protein kinases. Cell. 2007; 131:1248–1259. [PubMed: 18160036]

Truitt ML, Conn CS, Shi Z, Pang X, Tokuyasu T, Coady AM, Seo Y, Barna M, Ruggero D. Differential requirements for eIF4E dose in normal development and cancer. Cell. 2015; 162:59–71. [PubMed: 26095252]

Tsuneizumi K, Nakayama T, Kamoshida Y, Kornberg TB, Christian JL, Tabata T. Daughters against dpp modulates dpp organizing activity in Drosophila wing development. Nature. 1997; 389:627–631. [PubMed: 9335506]

Vinayagam A, Hu Y, Kulkarni M, Roesel C, Sopko R, Mohr SE, Perrimon N. Protein complex-based analysis framework for high-throughput data sets. Sci. Signal. 2013; 6:rs5. [PubMed: 23443684]

Wang SH, Elgin SC. Drosophila Piwi functions downstream of piRNA production mediating a chromatin-based transposon silencing mechanism in female germ line. Proc. Nat. Acad. Sci. USA. 2011; 108:21164–21169. [PubMed: 22160707]

Woolford JL Jr. Baserga SJ. Ribosome biogenesis in the yeast Saccharomyces cerevisiae. Genetics. 2013; 195:643–681. [PubMed: 24190922]

Xi R, Doan C, Liu D, Xie T. Pelota controls self-renewal of germline stem cells by repressing a Bam-independent differentiation pathway. Development. 2005; 132:5365–5374. [PubMed: 16280348]

Xue S, Barna M. Specialized ribosomes: a new frontier in gene regulation and organismal biology. Nat. Rev. Mol. Cell Biol. 2012; 13:355–369. [PubMed: 22617470]

Yan D, Neumuller RA, Buckner M, Ayers K, Li H, Hu Y, Yang-Zhou D, Pan L, Wang X, Kelley C, et al. A regulatory network of Drosophila germline stem cell self-renewal. Dev. Cell. 2014; 28:459–473. [PubMed: 24576427]

Zhang Q, Shalaby NA, Buszczak M. Changes in rRNA transcription influence proliferation and cell fate within a stem cell lineage. Science. 2014; 343:298–301. [PubMed: 24436420]

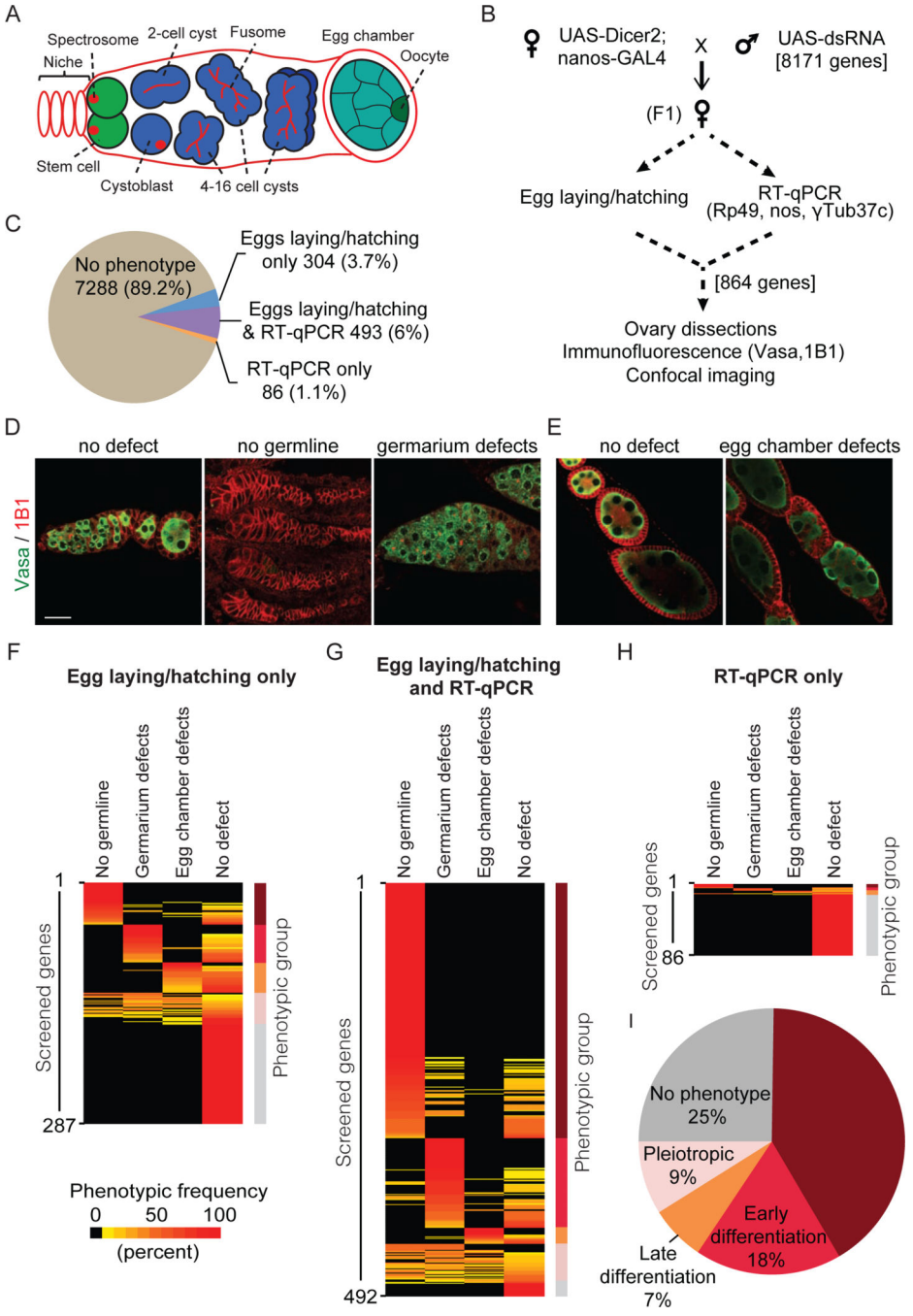

Figure 1. Transcriptome-wide *in vivo* RNAi screen: workflow and summary of results

(**A**) Schematic representation of the Drosophila germarium. (**B**) Screening crosses and workflow. For primary screening, 8171 genes were knocked down using transgenic RNAi lines and the germline-specific driver (*nos*-Gal4). For the secondary screen, crosses were repeated for 864 candidates. (**C**) Pie chart summarizing primary screen results. (**D-E**) Confocal images showing phenotypic categories. Ovaries were stained for Vasa (green) and 1B1 (red). (**F-H**) Heatmaps with phenotypic frequencies (black-yellow-red scale; 0-100%) observed for knockdowns of candidates. Phenotypic group classification, color-coded as in

(**I**), is indicated to the right of each heatmap. (**F**) Phenotypic results for candidates identified solely by egg laying/hatching, (**G**) by both RT-qPCR and egg laying/hatching or (**H**) exclusively by RT-qPCR assays. (**I**) Pie chart summarizing secondary screen results. Scale bars, 20 μM.

Related to Figures S1 and S2, and Tables S1 and S3.

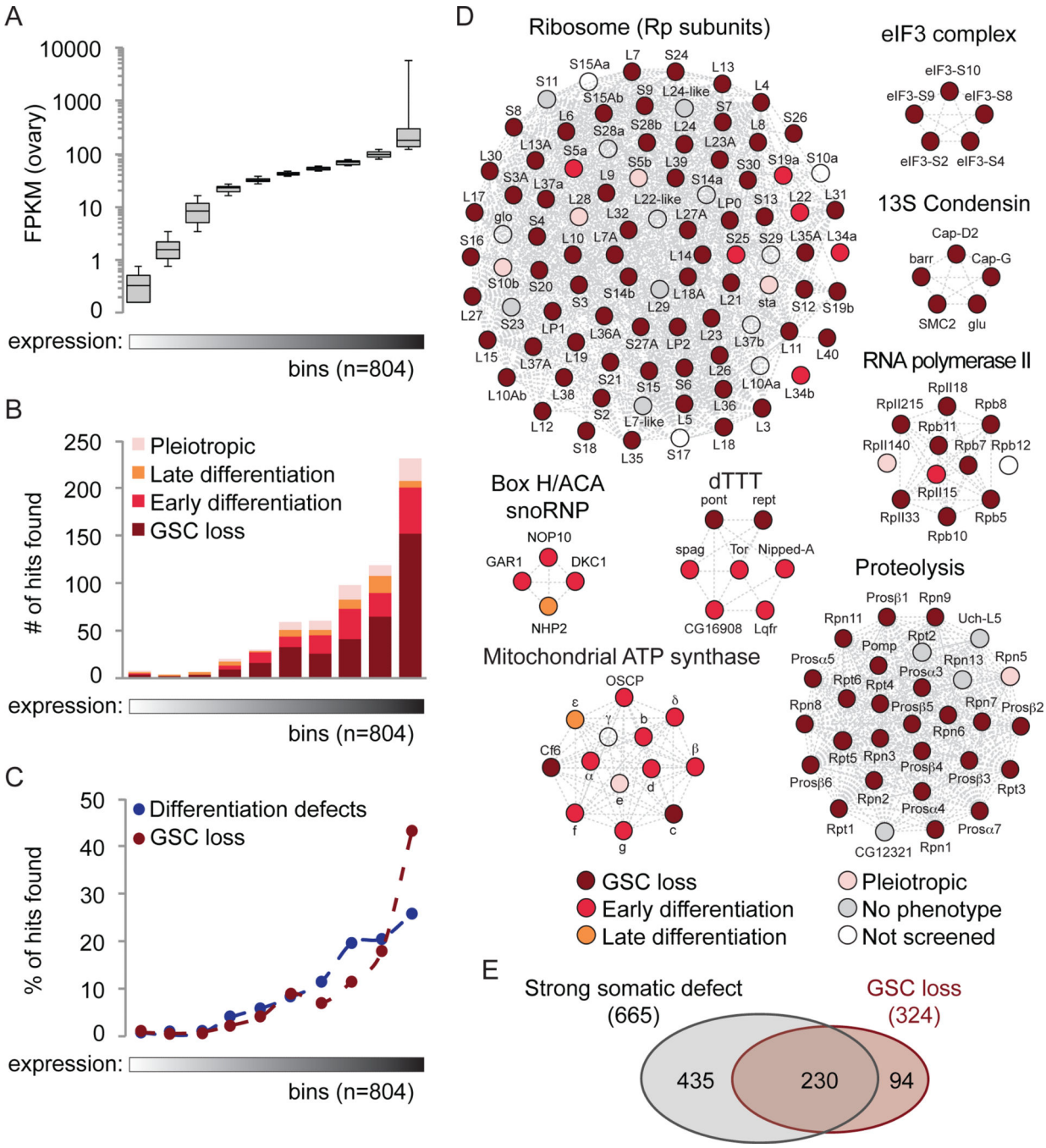

Figure 2. Germline maintenance factors are enriched for highly expressed genes functioning in core cellular networks

(**A**) Box plots displaying the distribution of screened genes according to their ascending expression level. Genes were organized into ten equal bins, each containing 804 genes. (**B**) The distribution of hits found in each of the expression bins defined in (**A**). (**C**) The percentage of hits showing either ‘GSC loss’ or ‘differentiation defects’ for each expression bin defined in (**A**). (**D**) Gene networks identified through COMPLEAT analysis (Table S2). Circles represent genes and colors indicate phenotypic classes as displayed in the bottom

panel. Gray lines designate protein interactions. (**E**) Venn diagram showing the overlap of 'GSC loss' genes and genes showing strong ovarian defects when knocked down in somatic ovarian cells (Handler et al., 2013).
Related to Figure S3 and Table S2.

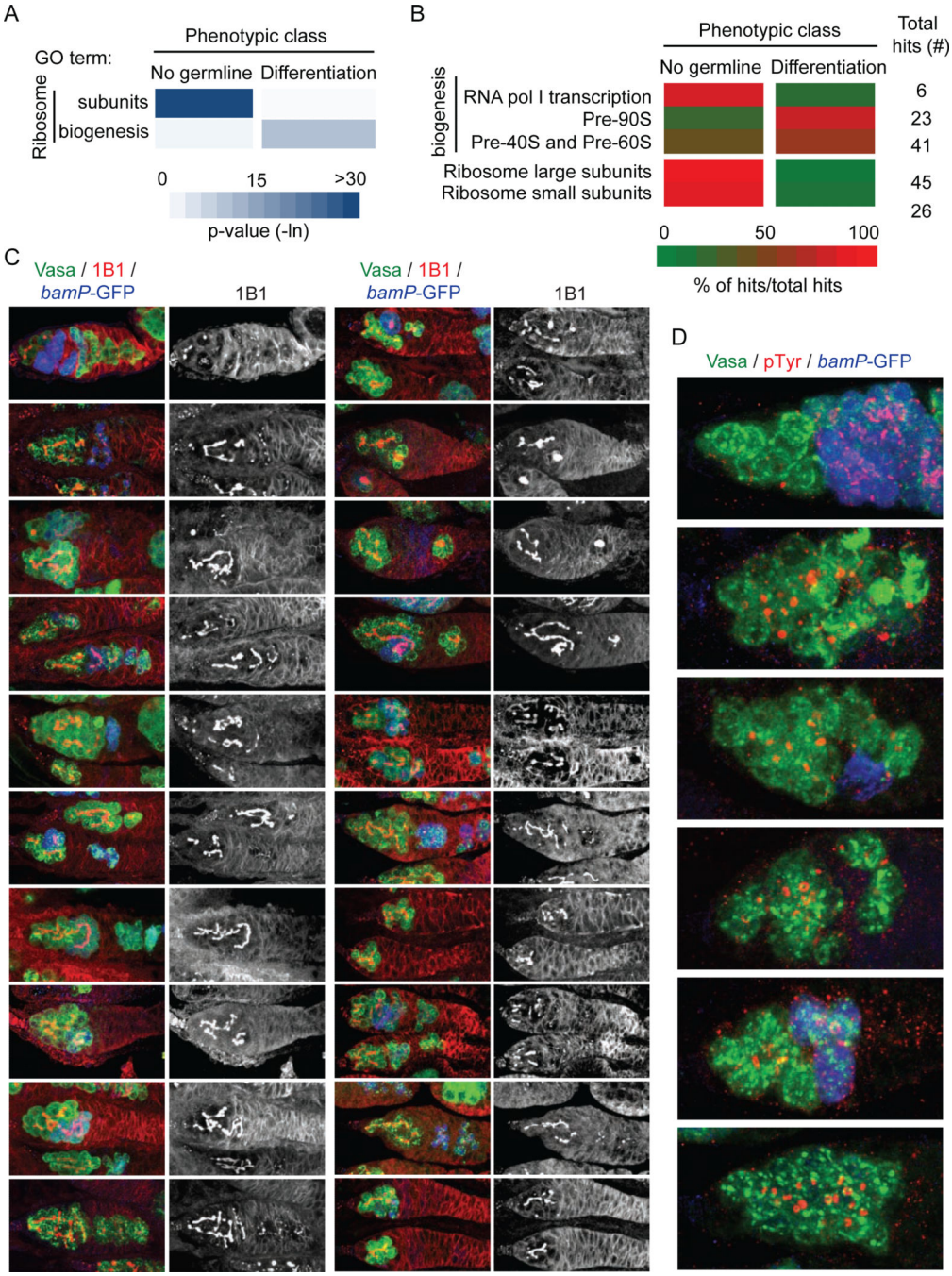

Figure 3. Knockdown of ribosome assembly genes causes 'stem cysts'

(**A**) GO term analysis for genes showing 'no germline' or 'differentiation' phenotypes (Table S2). *P*-values are shown in white to blue scale. (**B**) Frequency of 'no germline' and 'differentiation' hits (shown as a percent of hits from each category; green to red scale) for the different steps leading to ribosome biogenesis. Genes were annotated using the KEGG database. (**C**) Confocal projections of wild-type and RNAi knockdown germaria for genes involved in ribosome assembly and translation control. For convenience, we adopted yeast or mammalian nomenclature whenever homologs were clear (Woolford and Baserga, 2013).

Ovaries expressing BamP-GFP were stained for Vasa (green), 1B1 (red), and GFP (blue). Grayscale panels show 1B1. (**D**) Confocal projections of germaria stained for Vasa (green), phosphotyrosine (red; ring canal), and GFP (blue; BamP-GFP). Stars mark terminal filaments. Scale bars, 20 μM.

Related to Figures S4 and S5, and Table S2.

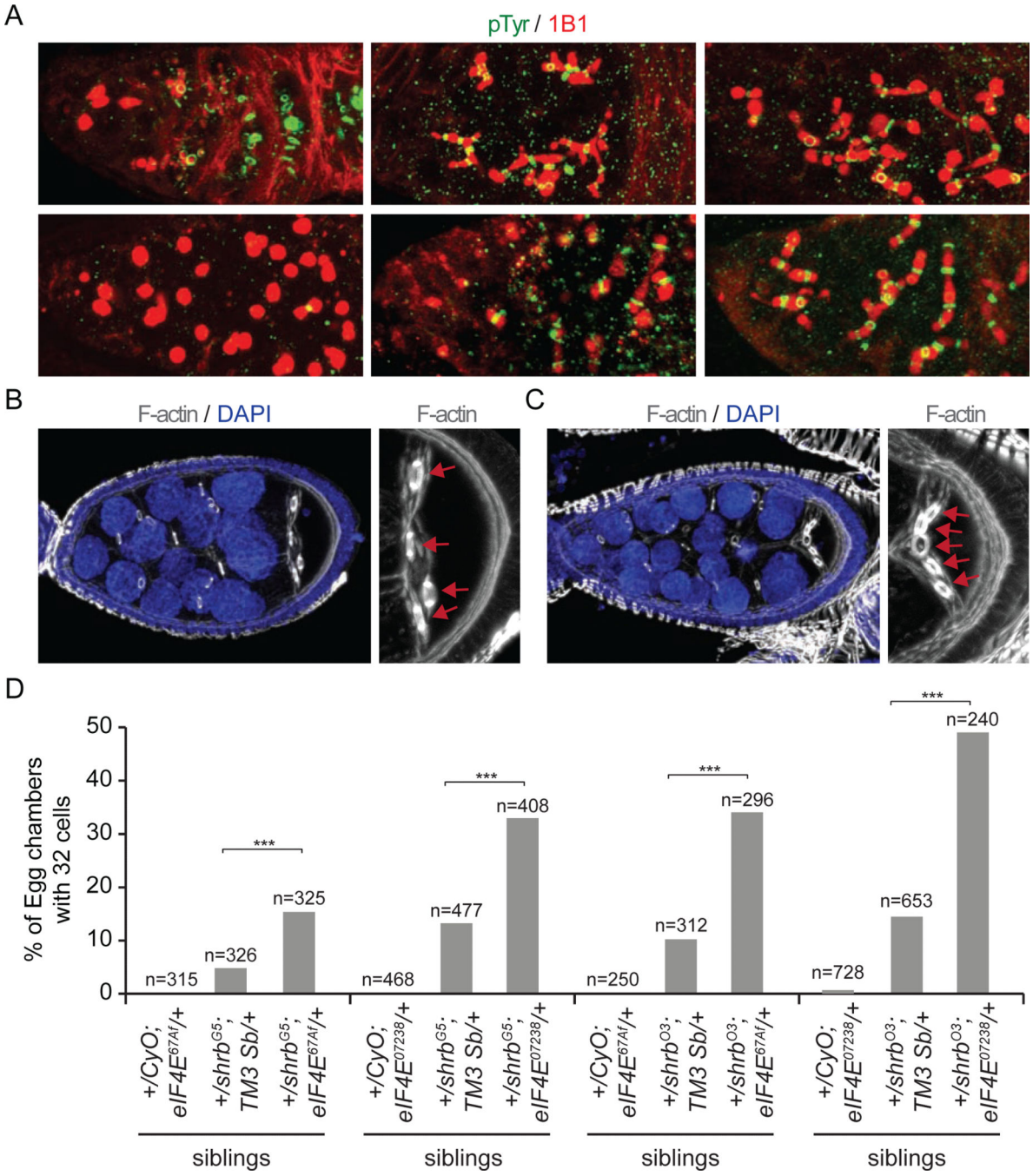

Figure 4. Ribosome assembly factors and eIF4E interact positively with the ESCRT-III protein Shrb to promote GSC abscission

(A) Confocal projections of germaria stained for 1B1 (red) and phosphotyrosine (green). Stars mark terminal filaments. (**B-C**) Confocal projections of (**B**) 16-cell and (**C**) 32-cell egg chambers. Ovaries were stained for Phalloidin (F-actin; grey) and DAPI (blue). Grayscale panels show F-actin channel in oocytes. Red arrows indicate ring canals connecting to the oocyte – four in 16-cell egg chambers and five in 32-cell egg chambers. (**D**) Frequency of egg chambers containing 32 cells in genetic interaction experiments. Sibling genotypes are described. *** represents Chi-square tests with $p<0.001$. Scale bars, 20 μM.

Related to Figure S5.

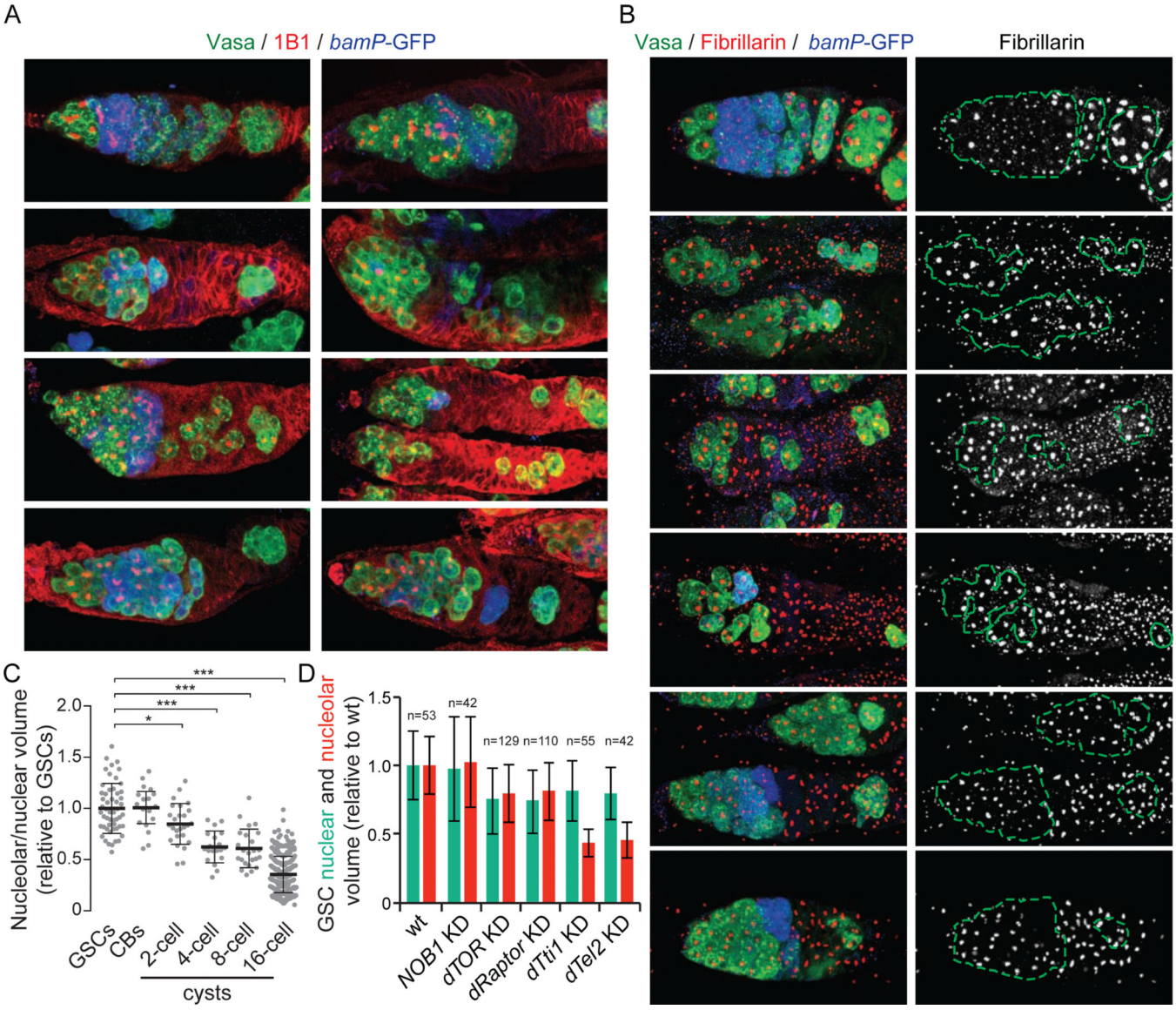

Figure 5. Knockdown of dTORC1 pathway and the cochaperone adaptors dTel2 and dTti1 affects GSC nucleolar hypertrophy and germline differentiation

(**A-B**) Confocal projections of germaria stained for (**A**) Vasa (green), 1B1 (red), and GFP (blue; BamP-GFP); or (**B**) Vasa (green), Fibrillarin (red, nucleolus), and GFP (blue; BamPGFP). (**B**) Grayscale panels show Fibrillarin. Germ cells are in green. (**C**) Quantification of nucleolar/nuclear volume ratio in wild-type germ cells (see experimental procedure). Results were plotted relative to GSCs. *** represents one-way analysis of variance with $p<0.001$ and * $p<0.01$. (**D**) Quantification of GSC nuclear and nucleolar volume in RNAi knockdowns. Results were plotted in relation to wild-type GSCs from measurement presented in figure 5C. Number of analyzed cells is presented at the top of each column. Data are represented as mean ± standard deviation. Scale bars, 20 μM.

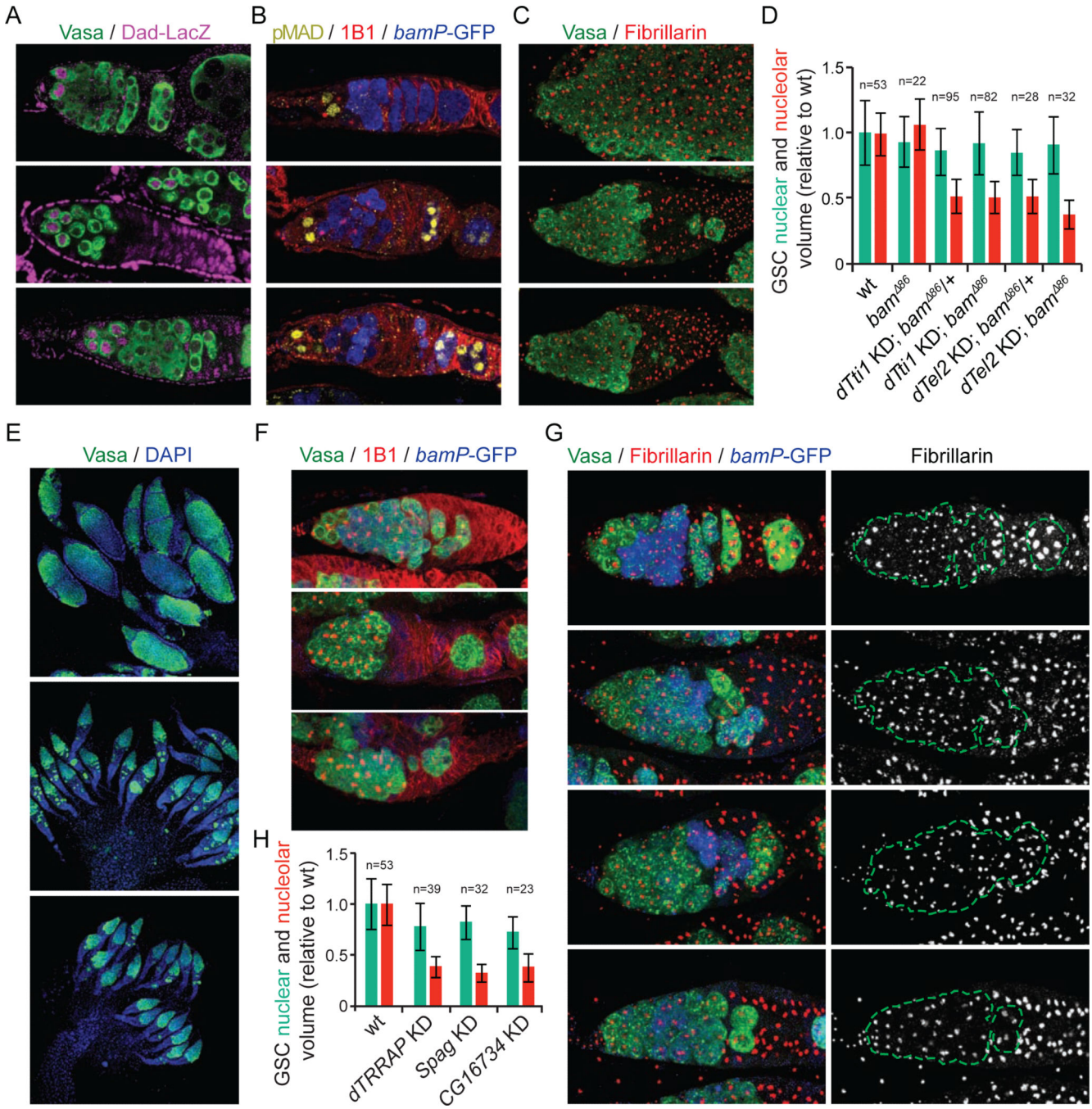

Figure 6. Phenotypic characterization of dTel2, dTti1, and their interactors

(**A**) Germaria carrying the *Dad-LacZ* reporter were stained for Vasa (green) and β-Galactosidase (magenta). (**B**) Germaria were stained for pMad (yellow, GSCs), 1B1 (red), and GFP (blue; BamP-GFP). (**C**) Confocal projections of germaria stained for Vasa (green) and Fibrillarin (red). (**D**) Quantification of GSC nuclear and nucleolar volume. Results were plotted in relation to wild-type GSCs from measurements in Figure 5C. Number of analyzed cells is at the top of each column. Data are represented as mean ± standard deviation. (**E**) Confocal projections of whole ovaries stained for Vasa (green) and DAPI (blue). (**F-G**)

Confocal projections of germaria stained with (**F**) Vasa (green), 1B1 (red), and GFP (blue; BamP-GFP); or (**G**) Vasa (green), Fibrillarin (red), and GFP (blue; BamP-GFP). (**G**) Grayscale panels show Fibrillarin. Germ cells are outlined in green. (**H**) Quantification of GSC nuclear and nucleolar volume in knockdowns. Results were plotted as in (**D**). Scale bars, (**A-C,F-G**) 20 μM, (**E**) 100 μM.

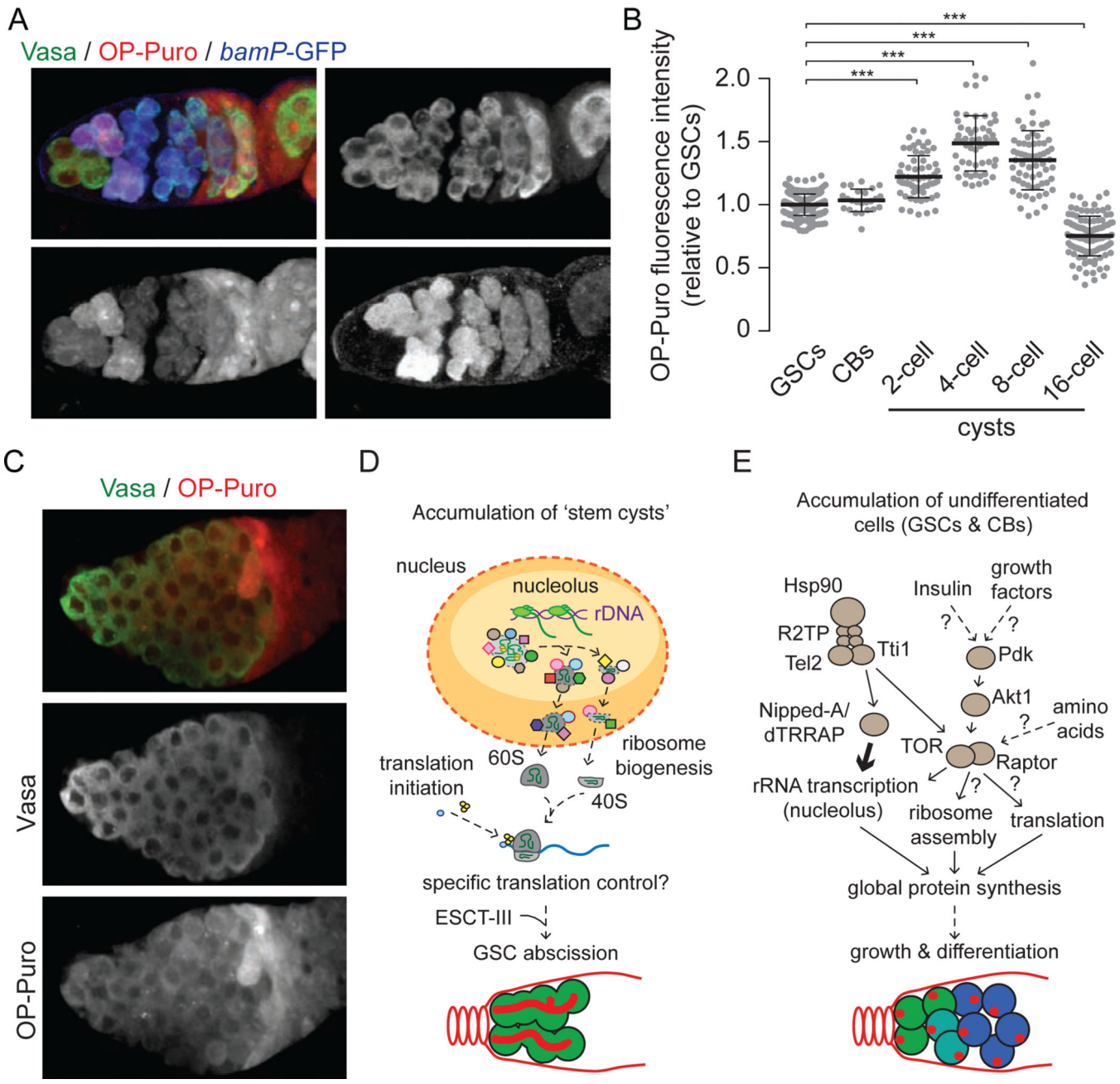

Figure 7. Protein synthesis during GSC differentiation

(**A**) Representative confocal image of protein synthesis analysis in wild-type germaria expressing BamP-GFP. Live ovaries were incubated with OP-Puro (red), and stained for Vasa (green) and GFP (blue). (**B**) Quantification of OP-Puro fluorescence intensities. Graph summarizes data for all time points (15, 30, 45, and 60 min; Figure S6A for individual analyses). *** represents one-way analysis of variance with $p<0.001$. (**C**) Representative confocal image of protein synthesis analysis in $bam^{\Delta 86}$ mutant ovaries. After labeling OP-Puro (red), ovaries were stained for Vasa (green). (**D**) Knockdown of ribosome assembly and translation initiation factors results in accumulation of germline 'stem cysts'. (**E**) Knockdown of genes positively regulating the function of the transcription co-factor

dTRRAP and the TOR kinase leads to the accumulation of undifferentiated cells (GSCs and CBs). Scale bars, 20 μM.
Related to Figure S6.